PROBING THE STRUCTURE OF COMETARY ICE

MICHAEL A. WILSON[1,2], ANDREW POHORILLE[1,2], PETER JENNISKENS[1] and DAVID F. BLAKE[1]

[1] *NASA Ames Research Center, Moffett Field, CA 94035, U.S.A.*

[2] *Department of Pharmaceutical Chemistry, University of California, San Francisco, CA 94143, U.S.A.*

(Received 3 December, 1993)

Abstract. Computer simulations of bulk and vapor deposited amorphous ices are presented. The structure of the bulk low density amorphous ice is in good agreement with experiments on pressure disordered amorphous ice. Both the low density bulk ice and the vapor deposited ices exhibit strong ordering. Vapor deposition of hot (300 K) water molecules onto a cold (77 K) substrate yields less porous ices than deposition of cold (77 K) water molecules onto a cold subtrate. Both vapor deposited ices are more porous than the bulk amorphous ice. The structure of bulk high density amorphous ice is only in fair agreement with experimental results. Attempts to simulate high density amorphous ice *via* vapor deposition were not successful. Electron diffraction results on vapor deposited amorphous ice indicate that the temperature of the nucleation of the cubic phase depends upon the amount of time between the deposition and the onset of crystallization, suggesting that freshly deposited ice layers reconstruct on times of the order of hours. The temperature dependence of the microporosity of the vapor deposited amorphous ices might affect laboratory experiments that are aimed at simulating astrophysical ices in the context of the origin of prebiotic organic material and its transport to the Earth.

1. Introduction

All theories of the origin of cellular life require the abiotic synthesis of reduced organic matter. Since organic compounds and their precursors appear to have been difficult to synthesize in the mildly reducing model of the prebiotic atmosphere favored by geochemists (for a discussion see Chang, 1993), an extraterrestrial source of prebiotic organic matter has been proposed as an alternative (e.g. Chyba *et al.*, 1990). Reduced carbon has an origin in intersellar space, where it is formed through UV photolysis of water ice mantles on interstellar grains and subsequent processing of radical recombination products (Greenberg *et al.*, 1972; Jenniskens *et al.*, 1993). Water ice is also capable of trapping carbon-containing impurities, like CO, CO_2, and CH_3OH, that thus become part of the solid bodies formed from interstellar grains – comets. During the early bombardment, impacting comets supplied the early Earth with an abundance of water, but the impact energy may have evaporated and oxidized most of their reduced carbon. Organic material was also delivered to the early Earth in the form of solid interplanetary dust particles (IDPs), which were released from comets in the inner solar system. IDPs rained onto the early Earth with a flux decreasing in time from 10^9 to 10^5 kg yr^{-1} (Anders, 1989). For a good understanding of the composition of these early impactors and the composition of ice mantles in interstellar grains, it is necessary to know the trapping efficiencies and outgassing properties of astrophysical ices (Laufer *et al.*, 1987).

Origins of Life and Evolution of the Biosphere **25:** 3–19, 1995.

Ice in space can be formed by vapor deposition at low temperature (T < 100 K). Vapor deposited water ice has been studied since 1935 (Burton and Oliver, 1935) and a non-ending stream of papers is a testament to its intriguing properties. It consists essentially of a random tetrahedrally-bonded network, but has unique properties because this network is hydrogen bonded. For example, vapor deposition of water results in a microporous ice (Mayer and Pletzer, 1986), in which the hydrogen-bond network is quickly restructured possibly due to the presence of 5-coordinated oxygen (Sciortino *et al.*, 1992). Three structurally distinct forms of vapor-deposited amorphous water ice are observed at low pressure and temperature-high density ice (I_ah) (Narten *et al.*, 1976, Jenniskens and Blake, 1994), low density ice (I_al) (Burton and Oliver, 1935), and a recently identified form which coexists with crystalline cubic ice (I_ac) (Jenniskens and Blake, 1994). High and low density amorphous ices can also be formed from pressurizing bulk hexagonal ice I_h (Mishima *et al.*, 1984), and these ices appear to differ from the vapor deposited ices such that they are usually referred to as HDA and LDA ice, respectively.

Many questions remain related to radical diffusion in UV photolyzed ices, the trapping properties of the vapor deposition process, and the release of impurities upon heating of the ice. In the absence of samples of astrophysical ice, these questions are being studied by generating its analogs in laboratory experiments. However, these experiments are hampered by time-, annealing-, and deposition-rate dependencies. In addition, it is often impossible to reproduce astrophysical conditions during deposition experiments. Notably, the rotational and translational energies of molecules deposited in the laboratory are usually much higher than those which exist under astrophysical conditions. The consequences of these differences are not known. In order to understand the trapping properties of the vapor deposition process, the physical behavior of amorphous ice as a function of temperature, and the relation between astrophysical and laboratory-generated ice structures, we have studied amorphous ice systems using molecular dynamics (MD) computer simulations. This paper presents numerical results for amorphous, pure water ice. We will discuss the bulk structures of the low-density and high-density ices, and the microporous structure formed during simulated vapor deposition. The changes in microporosity will be examined as a function of temperature.

2. Method

In an MD simulation, the equations of motion of the system are solved numerically, and the properties of interest are obtained from averages over the resulting numerical trajectories. The majority of MD calculations are based on classical mechanical models, and the problem reduces to the solution of Newton's equations of motion for a system of interacting atoms and/or molecules. Detailed descriptions of this method can be found in a number of basic texts (Allen and Tildesley, 1987; see also Pohorille and Wilson, 1994, this volume).

Several models are available to describe the interactions between water molecules. We have selected the TIP4P model (Jorgensen *et al.*, 1984) because it provides a good description of liquid water, as found through the comparison of the water-water pair correlation functions with the results of neutron scattering experiments, as well as the liquid-vapor interface of water (Wilson *et al.*, 1987, 1988). The TIP4P model can also reproduce many physical properties of crystalline ices (Tse and Klein, 1988), and the pressure disordered high (HDA) and low (LDA) density amorphous ices (Tse and Klein, 1990). Related studies on solid amorphous ice phases have been done using the ST2 model of water (Poole *et al.*, 1992), and amorphous ice clusters using the TIPS2 model (Zhang and Buch, 1990a b; Buch, 1990, 1992).

The emphasis here is on the vapor deposition process, which requires appropriate substrates of low and high density amorphous ices. These were produced from bulk configurations of HDA and LDA ices. To produce statistically representative configurations of bulk LDA and HDA ices, we used a strictly computational procedure called quenching. While quenching does not correspond directly to any physical process, it has some similarities to pressure deformation of hexagonal ice at low temperature. The same procedure has been used previously to generate aqueous glasses from liquid water configurations (Pohorille *et al.*, 1987).

Both LDA and HDA ice were obtained by quenching configuration drawn from MD simulations of water at 300 K to the desired temperatures of 77 K and 10 K, respectively. In each case, the system consisted of 343 water molecules placed in a cubic simulation box. To eliminate undesirable boundary effects periodic boundary conditions were used. The density of water for the production of LDA and HDA was set to the experimental values of, 0.94 g/cc and 1.17 g/cc, respectively (Narten *et al* ., 1976). After equilibrating the system for 100 ps, an MD trajectory of 1 ns was generated at an elevated temperature (300 K). 100 configurations uniformly spaced along the trajectory were saved for quenching. The HDA ice configurations were generated by steepest descent minimization of the high density water configurations, which guides the system into the nearest local energy minimum. A steepest descent quench was also tried for the LDA ice, but was not successful because rapid quenching disrupts the hydrogen bond network. Instead, formation of the LDA ice structure required gentle quenching in stages. Each stage consisted of a 25 ps trajectory during which the temperature was reduced by 50 K, followed by 25 ps of equilibration. In the last stage, the temperature was lowered from 100 to 77 K.

The vapor deposition simulations required a substrate with a free amorphous ice-vapor interface. This system was created from a quenched configuration of bulk amorphous ice by instantaneously expanding one dimension of the simulation box (see Figure 1). This generated an ice lamella with two free surfaces in the middle of the simulation box. Since the bulk configuration was not a representative equilibrium configuration for the new geometry the system was annealed to maintain

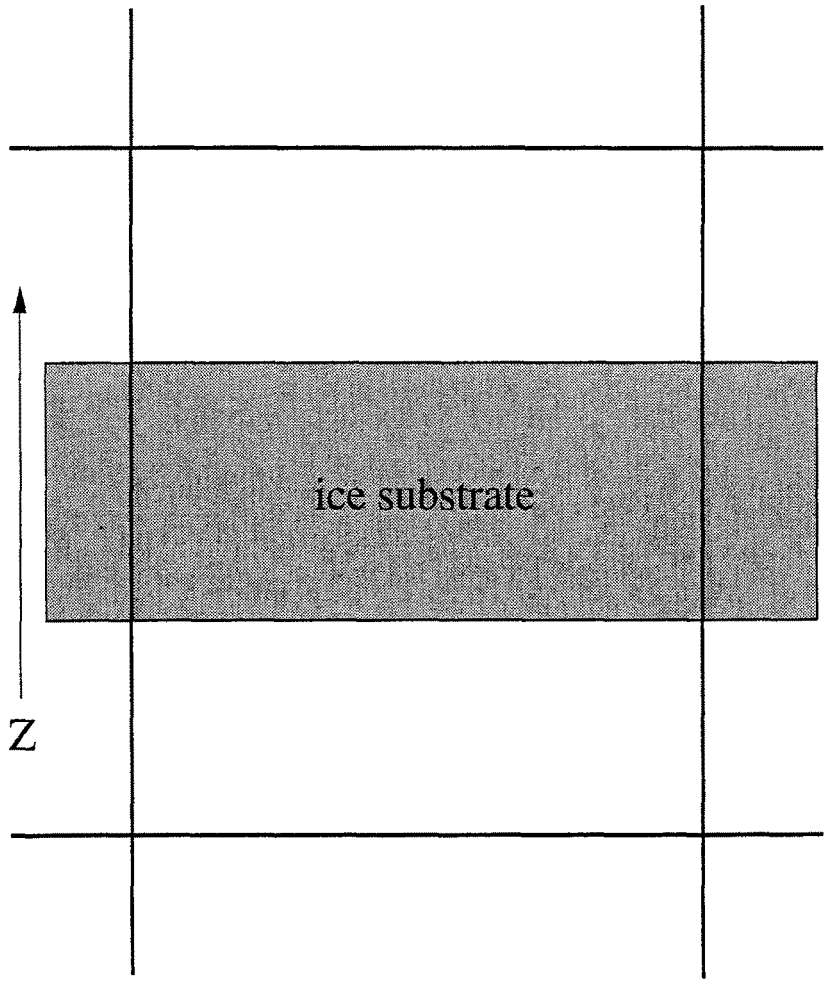

Fig. 1. Schematic drawing of the water substrate. The boundary conditions in the z-direction have been removed, giving two solid-vapor interfaces. The boundary conditions in the x- and y-directions remain, giving the system a semi-infinite lamellar geometry.

the correct temperature. An annealing trajectory of 50 ps at 77 K was generated to equilibrate the LDA ice substrate. The HDA ice substrate was annealed at 10 K.

The vapor deposition runs were carried out by inserting two water molecules into the system, one above the upper surface and the other below the lower surface. The initial x- and y-positions (parallel to the ice lamella) of the molecules were chosen randomly. The z-positions were chosen such that each of the inserted molecules was at least 8 Å from the closest water molecule of the lamella. The velocities of the incoming molecules were sampled from the Maxwell–Boltzmann distribution at the required temperature, with the restriction that the initial velocity in the z-direction pointed toward the surface. A normal MD trajectory was generated for

the first 8 ps. Then, the velocities of all the molecules were sampled from the Maxwell–Boltzmann distribution at the equilibrium temperature of the substrate every 0.25 ps for 2 ps. Sampling of velocities is necessary because water molecules from the vapor phase are attracted to the surface with an energy of about 8 kcal/mol, which is converted to thermal energy when they collide with the substrate. Under experimental conditions, the heat is distributed into a reservoir formed by a large number of molecules in the substrate. However, our microscopically-sized substrate would have become substantially hotter after just a few deposition events if the resampling of velocities had not been performed.

A total of 5 vapor deposition simulations have been carried out. These included deposition of water molecules at 77 K and 300 K onto an LDA substrate at 77 K, and deposition of water molecules at 10 K and 300 K onto an HDA substrate at 10 K. For the deposition of molecules at 77 K onto the LDA substrate, two separate runs were performed. The depositions onto the low density substrate were designed to investigate conditions similar to those in laboratory experiments (300 K molecules impinging on a 77 K substrate) and conditions more appropriate to astrophysical ice formation (77 K molecules impinging on a 77 K substrate). A substrate temperature of 77 K was chosen because recent neutron scattering results for low density ice were obtained at this temeprature (Bellissent-Funel *et al.*, 1987). The deposition simulations at 10 K were designed to model both the conditions under which interstellar ices form (10 K molecules onto a 10 K substrate) and experimental conditions (300 K molecules onto a 10 K substrate). An HDA substrate was used in the simulations because experimental vapor deposition results at this temperature indicate that the resulting ice is I_ah (Narten *et al.*, 1976; Jenniskens and Blake, 1994).

3. Results

3.1. Bulk structural features

The quenching procedure resulted in a good representation of LDA ice, but only a fair representation of HDA ice. The neutron weighted pair correlation functions for the simulated bulk LDA and HDA ices are shown in Figure 2. Since these are bulk samples, the results are compared with experimental results on bulk amorphous ice formed from pressure disordered hexagonal ice I_h (Bellissent-Funel *et al.*, 1987). The main differences between the two amorphous forms found experimentally are well reproduced by the computer simulation. The neutron weighted pair correlation functions are also in fair agreement with those obtained from extensive calculations on the phase behavior of bulk ST2 water (Poole *et al.*, 1992).

The hydrogen bonding character of the ices can be seen clearly in Figure 3, which shows the oxygen-oxygen, oxygen-hydrogen, and hydrogen-hydrogen radial distribution functions (RDFs) for the LDA and HDA forms. The height and location of the first and second peaks in the oxygen-oxygen RDF is indicative of the tetrahedral ordering found in liquid water. This result is in good agreement with

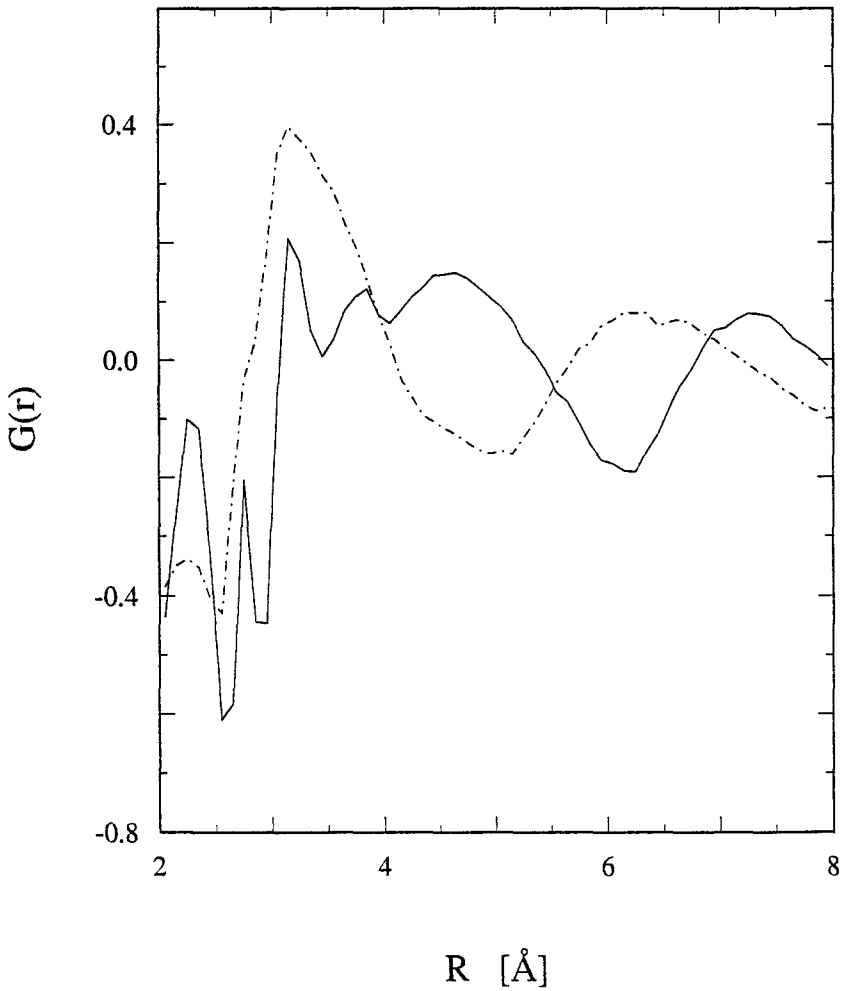

Fig. 2. Neutron-weighted pair correlation functions from bulk quenches of LDA (solid line) and HDA ice (dot-dash line). The neutron-weighted pair correlation function, $G(r)$, is related to the usual atom-atom radial distribution functions by $G(r) = 4\pi\rho r \times (0.092G_{O-O}(r) + 0.422G_{O-H}(r) + 0.486G_{H-H}(r)-1)$ where the numerical coefficients are scattering weights associated with the neutron scattering experiments.

X-ray diffraction results on pressure induced LDA ice (not shown) (Bizid *et al.*, 1987). The main difference between the computer simulation results and the X-ray data is that the first peak is much broader in the X-ray data, which suggests that the computer simulated ices may not be fully relaxed.

In contrast, the first peak in the oxygen-oxygen RDF of HDA ice is smaller and broader than for LDA ice, and the rest of the structure is washed out, indicating a greatly distorted hydrogen bond network. The X-ray results on HDA ice also show substantially less structure than the LDA ice. However, the agreement between the RDF of the computer simulated HDA ice and the X-ray diffraction results

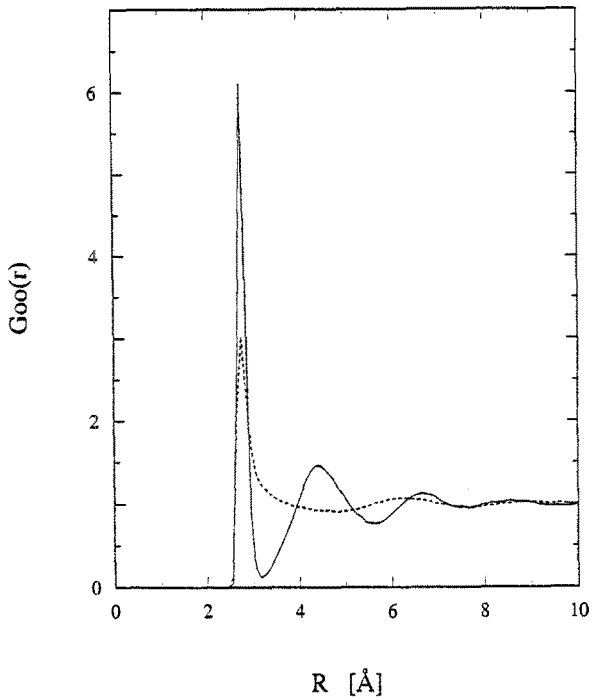

Fig. 3a.

Oxygen-Oxygen radial distribution functions for bulk LDA ice (solid line) and bulk HDA ice (dot-dashed line).

(Bizid *et al.*, 1987) is only qualitative. In particular, the X-ray RDF of the HDA ice exhibits two next-nearest neighbor peaks at 3.7 and 4.65 Å, of which the 3.7 Å is presumably due to the presence of interstitial water molecules (Norten, *et al.*, 1976). This feature is absent in simulated HDA ice. We note that the lesser degree of ordering in the HDA ice is not simply an artifact of the rapid quenching procedure through which it was formed, since similar quenching of liquid water at a density of 1.0 g/cc yields a strongly ordered glassy structure (Pohorille *et al.*, 1987).

Integration of the area under the first peak in the oxygen-oxygen RDF obtained from the simulations yields a coordination number of 4.0 for LDA ice and 4.8 for HDA ice. Since the calculated HDA ice RDF does not have a well defined minimum beyond the first peak, the integration was truncated at 3.15 Å, which is the location of the minimum for the LDA form.

3.2. Vapor Deposition Simulations

In all vapor deposition simulations, ice structures with varying degrees of micro-porosity were obtained. Figure 4 shows density histograms of the water molecules

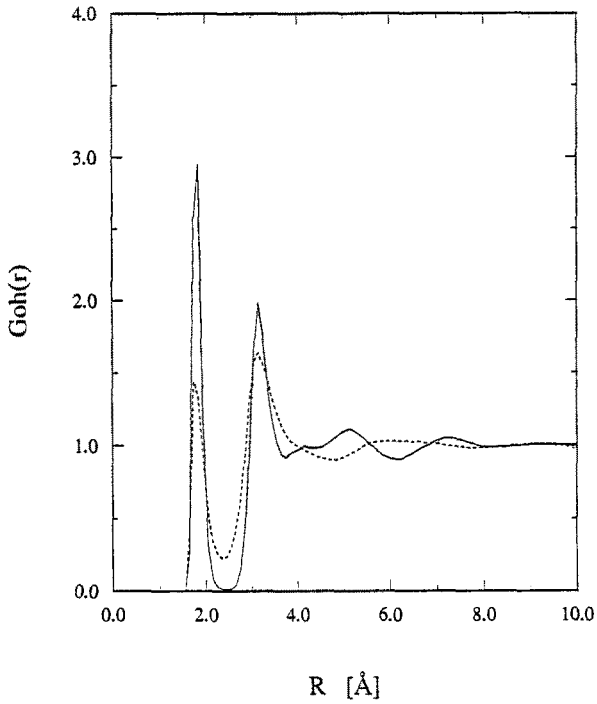

Fig. 3b.

The same but for the Oxygen-Hydrogen radial distribution functions.

obtained from the deposition of water molecules at 300 K onto a 77 K LDA ice substrate for several intermediate stages during the simulation. The substrate occupies the region from 0 Å to about 11 Å, and no noticeable changes in the density of the substrate were observed during the deposition. The density in the range 11 to 20 Å is fairly large, about 0.9 g/cc, and remains stable after 250 deposition events. Then, the density profile drops sharply and exhibits a second plateau region between 20 and 35 Å, with a density of about 0.6 g/cc. The decrease in density is due to the formation of micropores within the deposited ice layer, and is not the result of an open but corrugated surface.

The influence of the initial kinetic energy of the water molecules during deposition was tested by depositing molecules at 77 K onto a 77 K LDA ice substrate. The density histograms after 200 deposition events are shown in Figure 5. By comparing these results with Figure 4 we can gauge the effect of the initial thermal energy of water molecules in the vapor phase on the resulting ice structure. The deposition of the colder water molecules leads to the formation of a less dense ice structure, containing markedly larger micropores. Even though the formation of these pores is energetically unfavorable, the system is trapped in a local minimum

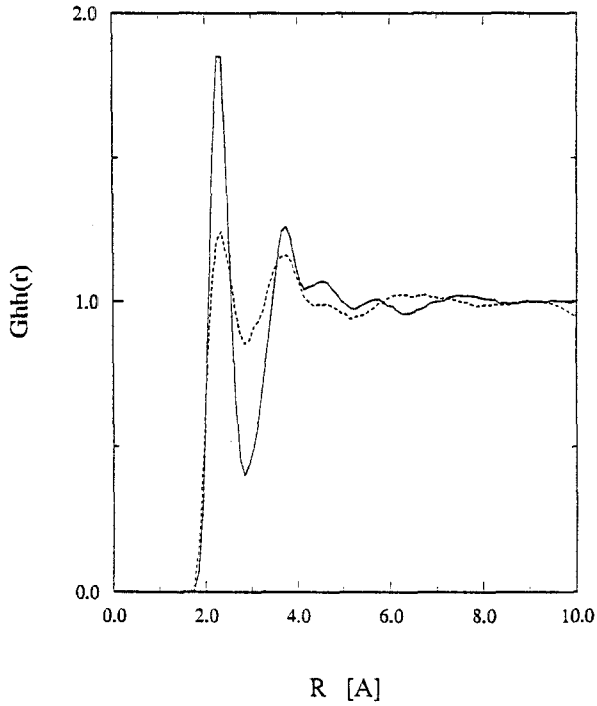

Fig. 3c.

The same but for the Hydrogen-Hydrogen radial distribution functions.

of the potential energy, and incoming molecules do not carry sufficient energy to displace the system from this local minimum. Thus, the system does not possess enough thermal energy to allow the surface to reconstruct. The density histogram of the system in which the water molecules impinge at 300 K indicates that the hotter molecules do have enough energy to allow a more extensive reconstruction of the surface after the collision. This implies that significant reconstruction usually occurs over the short time scales in laboratory experiments, but not in the astrophysical conditions they model.

In interstellar space, deposition may occur at substrate temperatures as low as 10 K. At these temperatures, laboratory experiments show the formation of a high density amorphous layer of ice $I_a h$. We carried out a deposition on a substrate at 10 K of both warm (300 K) and cold (10 K) water molecules. In neither case were we able to observe a high density amorphous layer. Rather, both experiments yielded the tetrahedral structure of the lower density amorphous ice. The very cold substrate temperature led to a more microporous structure, because the system had even less energy available for surface reconstruction than at 77 K.

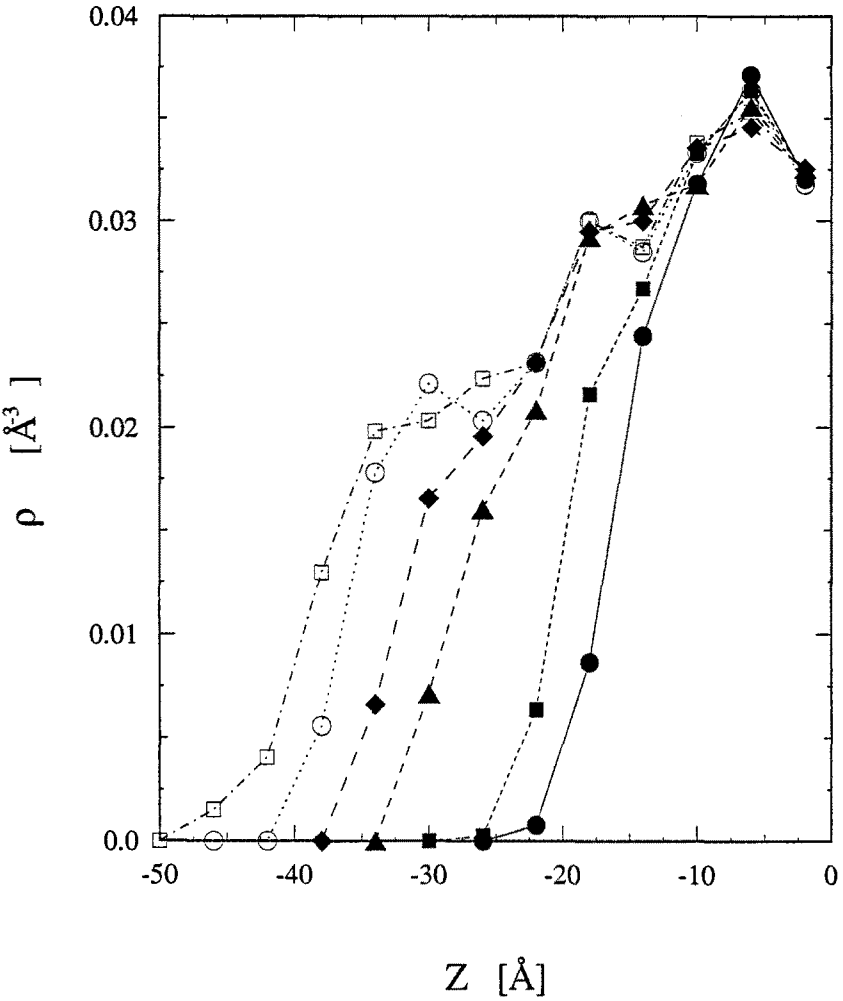

Fig. 4. Density histograms from the deposition of water molecules at 300 K onto the LDA ice substrate at 77 K for several intermediate stages of the deposition experiment. The lamellar geometry from Figure 1 has been averaged over both surfaces of the lamella, so the initial substrate is in the region 0–12 Å. The filled circles show the density profile after 100 depositions. The filled squares, filled triangles, filled diamonds, open circles and open squares show the density profiles after 150, 250, 300, 350, and 400 deposition events, respectively. The profiles are calculated with a resolution of 4 Å, and the lines are drawn between the points only as a guide.

Qualitatively, the structure of the deposited ice is more porous than the substrate. The porous structures of the substrate and the vapor deposited layer are extremely stable over the time scales of the computer simulations, and substantial changes in the densities can only be achieved by heating the system. Heating the ice layer deposited at 77 K with 300 K water caused the collapse of the microporous structure, but only above 150 K. Very little change was observed in the structure over times of 250 ps at 100, 125, and 150 K. When the temperature was raised to 175 K,

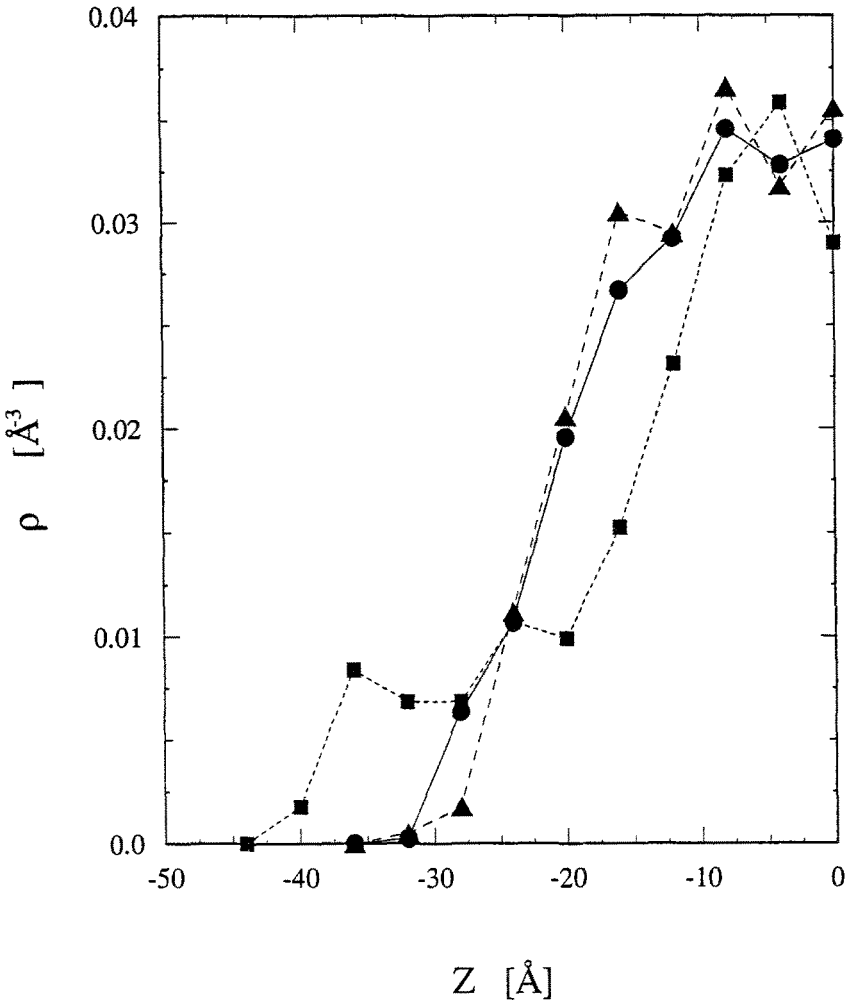

Fig. 5. Density histograms for three runs using the LDA ice substrate at 77 K. The circles are for a run with the impinging molecules at 77 K after 200 depositions. The squares are for a second run, also with the impinging molecules at 77 K. The triangles are with the impinging molecules at 300 K. The profiles are calculated with a resolution of 4 Å, and the lines are drawn between the points only as a guide.

the system became more compact as the voids in the structure collapsed, and the density approached the density of the substrate. While the micropores collapsed upon warming, the local order remained the same, as can be seen by comparing RDFs at 100 K with those at 175 K, shown in Figure 6. We note that the RDFs of the vapor deposited low density amorphous ice are in good agreement with the X-ray scattering results on vapor deposited amorphous ice at 77 K Narten, *et al.*, 1976).

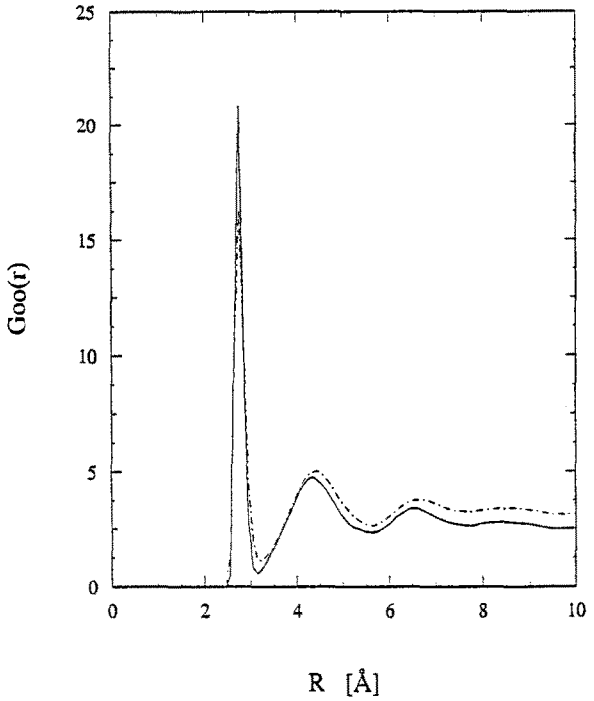

Fig. 6a.

Oxygen-Oxygen radial distribution functions from a vapor deposition experiment annealed at 100 K (solid line) and at 175 K (dot-dashed line).

4. Discussion

The most distinctive feature of the $I_a l$ ice obtained by computer simulation of vapor deposition is its microporosity. Voids in the ice structure develop through the formation of 'hills' separated by 'valleys' at the surface, which is not followed by extensive surface reconstruction. Once a valley begins to develop in the growing ice layer, the probability of depositing a water molecule into this region decreases. In effect, the water molecules on the hills around the valley tend to shroud it from incoming molecules. After enough water molecules have been deposited, the hills can broaden closing access to the valley, thereby creating a void in the ice structure. Our results are consistent with computer simulation results on amorphous ice clusters, which initially have a very open structure exhibiting dangling OH bonds, but become more dense upon annealing (Buch and Devlin, 1991). Similar effects have been observed in computer simulations of amorphous silicon films (Luedtke and Landman, 1989), even though no hydrogen bonding takes place in this system.

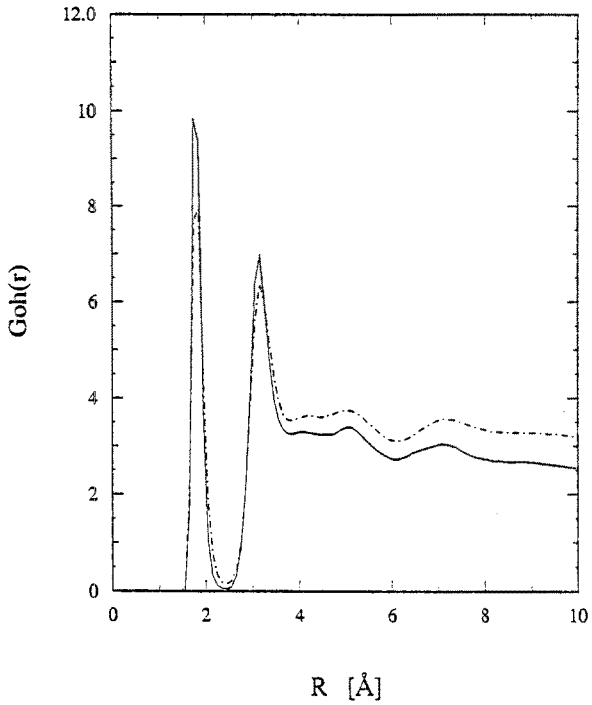

Fig. 6b.

The same for the Oxygen-Hydrogen radial distribution function.

The presence of microporosity in vapor deposited ices has been shown by nitrogen adsorption experiments (Mayer and Pletzer, 1986). Directly after deposition at 77 K, I_al has an effective surface area as high as 200–400 $m^2\ g^{-1}$. Heating for several minutes at 113 K results in the decrease of this surface area to some 40 $m^2\ g^{-1}$. Similarly, infrared spectroscopic studies of amorphous ice indicate that there are dangling OH bonds (in which the H does not participate in hydrogen bonding) in vapor deposited amorphous ice at 15 K, which diminish upon annealing to 60 K (Rowland and Devlin, 1991). Also, gradual changes in the dielectric permittivity of vapor deposited ice in the 77–130 K range have been attributed to a decrease of microporosity (Johari *et al.*, 1991). Amorphous ice formed via vapor deposition exhibits a much greater porosity than does hyperquenched water (Johari *et al.*, 1991).

An important concern in a direct comparison of the computational results with astrophysical and laboratory observations is whether or not the simulation time is sufficiently long to allow the ice network to restructure. If time scales of simulations are too short, the degree of microporosity predicted for the vapor deposited I_al ice could be markedly overestimated. The problem of time scales at low temperatures

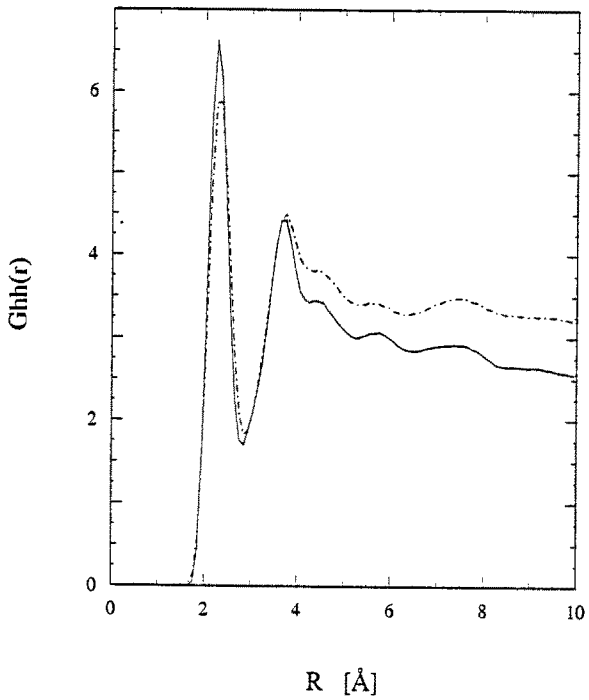

Fig. 6c.

The same for the Hydrogen-Hydrogen radial distribution function.

is further underscored by our inability to form high density ice during deposition at 10 K, a difficulty also experienced in computer simulations of ice clusters (Zhang and Buch, 1990a, b; Buch, 1990, 1992). The formation of I_ah by vapor deposition may involve extensive rearrangements of water molecules at the surface on time scales that are currently beyond the reach of MD simulations. However, it is also possible that at very low temperatures, quantum mechanical tunneling effects become important, and these have been neglected in the present computer simulations.

Additional complications to the time-scale problem have been brought to light by our recent laboratory experiments which indicate that the structure of the amorphous ice changes for over an hour after deposition. In a series of electron diffraction experiments on amorphous ices, it was found that the temperature at which the ice phase nucleates depends upon the amount of time the ice is annealed (Jenniskens and Blake, 1994). Figure 7 shows the temperature of crystallization as a function of annealing times. For longer times, both the temperature at which the cubic ice phase forms and the temperature at which the water is lost due to sublimation increase, indicating that the amorphous ice layer relaxes very slowly. Furthermore,

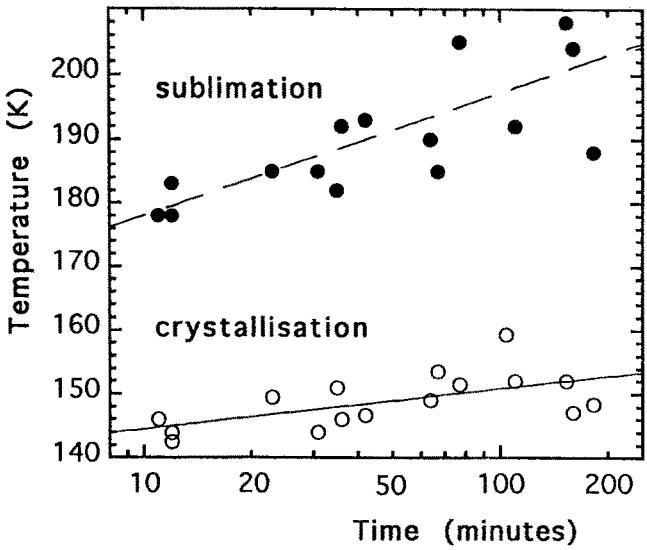

Fig. 7. Transition temperatures from amorphous to cubic ice as a function of the annealing time before nucleation. The open circles are the temperature at which the nucleation begins, and the filled circles are the temperature at which water sublimates.

this relaxation depends upon the time, but not the temperature at which the annealing is carried out. This suggests that the relaxation of the initial layer proceeds by a non-activated process, perhaps quantum mechanical tunneling or an entropy bottleneck.

Both our experiments and our computer simulations show that laboratory simulations of prebiotic ice are difficult. The properties of low density amorphous ice depend on the method by which it is produced and on specific experimental conditions. These can result in differing degrees of microporosity, which does not affect the ordering of water molecules. If the differences were the results of ordering of the water molecules, it would affect the positions of the peaks in the RDFs. However, comparisons of RDFs obtained for the bulk LDA, vapor deposited and annealed ices clearly indicate that the positions of the peaks are practically identical. The peak heights for the RDFs of the annealed ice differ from those in the vapor depositied ice only because of the effect of thermal broadening and the increased average density. (The differences in the heights of the peaks between the bulk and vapor-deposited ice are due to different normalizations). These comparisons suggest that different low density amorphous ices may have differing degrees of microporosity, but essentially the same local order.

Another focus of our work is on the differences between conditions of vapor deposition in the laboratory and in the astrophysical environment, of which the most important aspect appears to be the temperature of the deposited water molecules. In laboratory experiments, molecules impinge on the surface at room temperature while molecules deposited in astrophysical conditions have the same low

temperature as the substrate. This difference appears to influence the degree of microporosity, as the resulting amorphous ice is denser for hotter incoming water molecules. One possible explanation for this temperature dependence is that the hotter water molecules possess enough kinetic energy to break at least two hydrogen bonds at the surface. This, in turn, allows the molecules in the collision region to reorient and the surface to reconstruct. At lower temperatures, less energy is available to break hydrogen bonds, and the degree of surface reconstruction is lower. The initial kinetic energies of the (rigid) water molecules at 300 and 77 K are 1.8 kcal/mol and 0.45 kcal/mol, respectively. As these molecules reach the ice surface, they gain an additional 4–7 kcal/mol, depending upon orientations, due to attraction to the substrate. Since the energy of a hydrogen bond is approximately 4–5 kcal/mol a greater fraction of the molecules which start at 300 K will possess enough kinetic energy when they reach the surface to break two hydrogen bonds. This hypothesis, however, will require more extensive testing.

5. Concluding Remarks

We have simulated the vapor deposition of water onto a water substrate and have found the resulting amorphous low density ice to be microporous. The size of the pores increases with decreasing substrate temperature and decreasing vapor molecule temperature. In particular, deposition using water molecules at 300 K yielded less porous structures than water molecules at 77 K. It was found that the porous structures collapsed to a compact form when the temperature was raised to 175 K. While the porosity depends upon the conditions of the deposition, all observed structures are consistent with a random tetrahedrally-ordered network characteristic of I_al ice. Attempts to simulate I_ah ice proved unsuccessful.

The amorphous ices generated in these computer simulations can be used to investigate the sticking probabilities of atoms and small molecules to the amorphous ice surfaces during deposition, and the temperature dependence of their mobilities within the amorphous ice during heating. This work is currently in progress. We expect that it will lead to a better understanding of the processes that govern the diffusion of radials in UV photolyzed ices and the outgassing properties of impurities in astrophysically relevant ice mixtures, which are related to the production and transport efficienty of prebiotic reduced carbon.

6. Acknowledgements

This work has been supported in part by a NASA – Ames/UC Santa Cruz Joint Research Initiative NCA2-604 and the Planetary Biology Branch of the NASA – Ames Research Center. Computer resources for this work were provided in part by the Numerical Aerodynamical Simulation (NAS) program. P. J. is a recipient of a National Research Council – ARC Research Associateship.

References

Allen, M. P. and Tildelsey, D. J.: 1987, *Computer Simulations of Liquids*, Oxford University Press, New York.

Anders, E.: 1989, *Nature* **342**, 255.

Bellissent-Funel, M.-C., Teixeira, J., and Bosio, L.: 1987, *J. Chem. Phys.* **87**, 2231.

Bizid, A., Bosio, L., Defrain, A., and Oumezzine, M.: 1987, *J. Chem. Phys.* **87**, 2225.

Buch, V.: 1990, *J. Chem. Phys.* **93**, 2631.

Buch, V. and Devlin, J. P.: 1991, *J. Chem. Phys.* **94**, 4091.

Buch, V.: 1992, *J. Chem. Phys.* **96**, 3814.

Burton, E. F. and Oliver, W. F.: 1935, *Proc. R. Soc. London Ser. A* **153**, 166.

Chang, S., 1993, 'Prebiotic Sybthesis in Planetary Environments', in *The Chemistry of Life's Origins*, J. M. Greenberg *et al.* (eds.), Kluwer, Dordrecht, The Netherlands, pp. 259–299.

Chyba, C., Thomas, P. J., Brookshaw, L., and Sagan, C.: 1990, *Science* **249**, 366.

Greenberg, J. M., Yencha,, A. J., Corbett, J. W., and Frische, H. L.: 1982, *Mem. Soc. Roy. des Sci. de Loege, 6e ser.* **3**, 425.

Jenniskens, P. and Blake, D. F.: 1994, *Science* (submitted).

Jenniskens, P., Baratta, G. A., Kouchi, A., de Groot, M. S., Greenberg, J. M., and Strazzulla, G.: 1993, *Astron. Astrophys.* **273**, 583.

Johari, G. P., Hallbrucker, A. and Mayer, E.: 1991, *J. Chem. Phys* **95**, 2955.

Jorgensen, W. L., Chandrasekhar, J., Madura, J. D. Impey, R. W., and Klein, M. L.: 1984, *J. Chem. Phys.* **79**, 926.

Laufer, D., Kochavi, E., and Bar-Nun, A.: 1987, *Phys. Rev. B* **36**, 9219.

Luedtke. W. D. and Landman, U.: 1989, *Phys. Rev. B* **40**, 11733.

Mayer, E. and Pletzer, R.: 1986, *Nature* **319**, 298.

Mishima, O., Calvert, L. D., and Whalley, E.: 1984, *Nature* **310**, 393.

Narten, A. H., Venkatesh, C. G., and Rice, S. A.: 1986, *J. Chem. Phys.* **64**, 1106.

Pohorille, A., Wilson, M. A.: 1994, *Origins Life Evol. Biosphere*, (this volume).

Pohorille, A., Pratt, L. R., LaViolette, R. A., Wilson, M. A., and MacElroy, R. D.: 1987, *J. Chem. Phys.* **87**, 6070.

Poole, P. H., Sciortino, F., Essmann, U., and Stanley, H. E.: 1992, *Nature* **360**, 324.

Rowland, B. and Devlin, J. P.: 1991, *J. Chem. Phys.* **94**, 812.

Sciortino, F., Geiger, A., and Stanley, H. E.: 1992, *J. Chem. Phys.* **96**, 3857.

Tse, J. S.: 1992, *J. Chem. Phys.* **96**, 5482.

Tse, J. S. and Klein, M.: 1988, *J. Phys. Chem.* **92**, 315.

Tse, J. S. and Klein, M.: 1990, *J. Chem. Phys.* **92**, 3992.

Wilson, M. A., Pohorille, A. and Pratt, L. R.: 1987, *J. Phys. Chem.* **91**, 4873.

Wilson, M. A., Pohorille, A., and Pratt, L. R.: 1988, *J. Chem. Phys.* **88**, 3281.

Zhang, Q. and Buch, V.: 1990a, *J. Chem. Phys.* **92**, 1512.

Zhang, Q. and Buch, V.: 1990b, *J. Chem. Phys.* **92**, 5004.